

Numerical simulation of masonry shear panels with distinct element approach

Y. Zhuge[†]

*School of Geosciences, Minerals and Civil Engineering, University of South Australia,
SA 5095, Australia*

S. Hunt[‡]

*School of Petroleum Engineering and Management, The University of Adelaide,
SA 5005, Australia*

(Received August 7, 2002, Accepted March 11, 2003)

Abstract. Masonry is not a simple material, the influence of mortar joints as a plane of weakness is a significant feature and this makes the numerical modelling of masonry very difficult especially when dynamic (seismic) analysis is involved. In order to develop a simple numerical model for masonry under earthquake load, an analytical model based on Distinct Element Method (DEM) is being developed. At the first stage, the model is applied to simulate the in-plane shear behaviour of an unreinforced masonry wall with and without opening where the testing results are available for comparison. In DEM, a solid is represented as an assembly of discrete blocks. Joints are modelled as interface between distinct bodies. It is a dynamic process and specially designed to model the behaviour of discontinuities. The numerical solutions obtained from the distinct element analysis are validated by comparing the results with those obtained from existing experiments and finite element modelling.

Key words: distinct element method; unreinforced masonry; shear wall; failure; numerical modelling.

1. Introduction

Unreinforced masonry (URM) is one of mankind's oldest building materials, and has been extensively used throughout Australia and other regions around the world due to its low cost and simple constructional technology. However, the history of past earthquakes has shown that masonry buildings suffer the maximum damage, and earthquake resistant design of masonry has become an important issue in Australia since the Newcastle earthquake in 1989. Masonry is not a simple material, it is composed of two materials in a geometric array - an assemblage of bricks set in a mortar matrix. The influence of mortar joints and bond as a plane of weakness is a significant feature which is not present in concrete and this makes the numerical modelling of masonry very difficult especially when seismic analysis is involved.

[†] Senior Lecturer

[‡] Lecturer

Finite element method is a very powerful numerical method for the analysis of structures and it has been used to model the behaviour of unreinforced masonry in the last two decades. For static analysis, either a one-phase (macro modelling of composite) material model or a two-phase (micro modelling of brick and mortar) material model has been used. To simplify the problem, a homogeneous one-phase finite element model which incorporates the nonlinear material behaviour has been adopted by many investigators, especially for dynamic analysis (Dhanasekar 1985, LaRovere 1990, Vratsanou 1991, Gambarotta and Lagomarsino 1997b, Zhuge *et al.* 1998). In the model, some investigators adopted a homogenisation procedure to incorporate the effect of mortar joints (Gambarotta and Lagomarsino 1997b). However, the weak joint behaviour, which dominates the local failure of masonry in many cases, could not be simulated well by a continuum model.

Due to the nature of the problem, a more complicated two-phase finite element model has been used by some researchers in recent years (Page 1978, Lotfi and Shing 1994, Lourenco 1996, Gambarotta and Lagomarsino 1997a). In the model, the bricks are modelled as continuum elements and the joints are modelled by line interface elements. However, such models undoubtedly made analysis more complex and it is nearly impossible to apply these models to the dynamic/seismic analysis of masonry. According to the author's knowledge, previous micro modelling of unreinforced masonry has been limited to static analysis only.

There are other numerical models available which are mainly used for Rock Mechanics, namely the Boundary Element method (BEM) and the Distinct Element Method (DEM), although they are not commonly used for structural analysis. In the BEM, approximations only occur on the boundary of the domain, whereas the solution inside will always satisfy the equilibrium exactly. Thus, the BEM is very well suited for more complex structures than regularly patterned masonry (Dialer 1992). In this paper, an alternative analytical model has been introduced which is based on the Distinct Element Method (DEM). With the DEM, a solid is represented as an assembly of discrete blocks. Joints are modelled as interfaces between the distinct bodies. It is a dynamic process which is specially designed to model the behaviour of discontinuities. Therefore, it is well suited for masonry structures. By using the DEM, the response of discontinuous media, such as unreinforced masonry, under both static and dynamic loading can be simulated.

The Distinct Element method was first introduced by Cundall (1971) and has been progressively developed over the past two decades. The method was implemented in the computer program UDEC (Itasca 2000) and its major application has been in the field of rock mechanics and mining engineering. However, it is interesting to notice the similarities in the general material behaviour of rock and masonry, as both could be classified as non-homogeneous, discontinuous materials. Therefore, it is possible to apply the newly developed analytical techniques for rock engineering to micro modelling of masonry and the Distinct Element Method found its usefulness here.

The first application of the DEM to model masonry, found in the literature, was by Dialer (1992) and Psycharis *et al.* (2000). Dialer (1992) applied the DEM to analyse a small-scale two-brick specimen under shear stress. However, no detailed results were presented due to the lack of joint material properties. Psycharis *et al.* (2000) applied DEM to investigate the stability of freestanding classical columns under earthquake excitation. A simplified 2D model was adopted and the deformability of the blocks was neglected. Their studies proved that the DEM is very efficient in simulating the progressive collapse of blocky type structures.

Formica *et al.* (2002) adopted a similar approach for the numerical modelling of masonry, where a discrete model was established based on a different formulation approach. In their model, bricks were modelled as rigid bodies and the mortar joints as straight interface elements. The solution

strategy was based on a mixed path-following approach. The model could not simulate the failure of bricks.

The DEM has also been applied by the authors to analyse the structural behaviour of unreinforced masonry (Zhuge 1998, 1999). Initially, a stress boundary was used, where the horizontal load was monotonically increased. However, neither the failure pattern nor the principal stress distribution compared well with the experimental or finite element results. In the present study, an improved model is introduced, where the stress boundary is replaced by a progressively increased displacement boundary. An automatic damping scheme is replaced by a local damping scheme which has been proved more suitable for the type of problem being analysed.

In this paper, a numerical model based on the DEM has been applied to simulate the response of an unreinforced masonry shear wall panel with and without an opening, where the experimental testing results are available. The Distinct Element Method formation is introduced first, together with an outline of the basic procedures involved. The material models for bricks and joints are discussed as well as the failure criteria for bricks and joints. The material properties and testing procedures of two unreinforced masonry shear walls are then briefly reviewed, followed by the numerical model built up. The analysis is performed and the results between the distinct element model and experiments and finite element model are compared and discussed.

2. 2D distinct element modelling of discontinuous media

Distinct Element Method has been progressively developed over the past two decades. Cundall (1971) first introduced the Distinct Element Method to simulate progressive movements in blocky rock systems and the model has been implemented into a computer program UDEC since then. DEM was primarily intended for analysis in rock engineering projects, ranging from studies of the progressive failure of rock slopes to evaluations of the influence of rock joints, faults, bedding planes, etc. (Itasca 2000). DEM simulates the response of discontinuous media subjected to either static or dynamic loading.

In the DEM method, a solid is represented as an assembly of discrete blocks. Joints are modelled as interface between distinct bodies. The contact forces and displacements at the interfaces of a stressed assembly of blocks are found through a series of calculations, which trace the movements of the blocks (Itasca 2000). At all the contacts, either rigid or deformable blocks are connected by spring like joints with normal and shear stiffness k_n and k_s respectively (Fig. 1). Similar to the Finite Element Method (FEM), the unknowns in the DEM are also the nodal displacements and rotations of the blocks. However, unlike FEM, DEM is a dynamic process and the unknowns are solved by the equations of motion. The speed of propagation depends on the physical properties of the discrete system. The solution scheme used by DEM is the explicit time marching scheme and it uses finite contact stiffness.

If the blocks are rigid, block displacements are calculated from out of balance moment and forces applied to the centre of gravity of each block. Resultant forces F include boundary forces applied to the edges of the block and gravity.

Newton's second law of motion is applied for each block:

$$\frac{\partial \dot{u}^{(t)}}{\partial t} = \frac{F^{(t)}}{m} \quad (1)$$

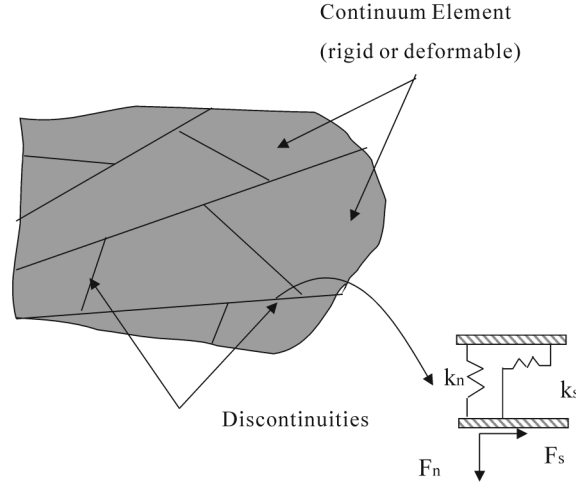


Fig. 1 Continuum and discontinuum elements in DEM

where \dot{u} is the velocity, m is the mass, and t is the time.

Following the central difference integration scheme, Eq. (1) can be transformed into:

$$\dot{u}^{(t+\Delta t/2)} = \dot{u}^{(t-\Delta t/2)} + \frac{F^{(t)}}{m} \Delta t \quad (2)$$

For blocks in two dimensions where we assumed several forces acting on the block (include gravity load), the velocity (Eq. 2) can be re-arranged which includes angular velocity of block:

$$\begin{aligned} \dot{u}_i^{(t+\Delta t/2)} &= \dot{u}_i^{(t-\Delta t/2)} + \left(\frac{\sum F_i^{(t)}}{m} + g_i \right) \Delta t \\ \dot{\theta}^{(t+\Delta t/2)} &= \dot{\theta}^{(t-\Delta t/2)} + \left(\frac{\sum M^{(t)}}{I} \right) \Delta t \end{aligned} \quad (3)$$

where $\dot{\theta}$ = angular velocity of block about centroid; I = moment of inertia of block; \dot{u}_i = velocity components of block centroid; $\sum M^{(t)}$ = total moment acting on the block; $\sum F_i^{(t)}$ = total force acting on the block; and g_i = components of gravitational acceleration.

Assume velocities are stored at the half-time step point, the new velocities in Eq. (3) can be used to determine the new block location:

$$\begin{aligned} x_i^{(t+\Delta t)} &= x_i^{(t)} + \dot{u}_i^{(t+\Delta t/2)} \Delta t \\ \theta^{(t+\Delta t)} &= \theta^{(t)} + \dot{\theta}^{(t+\Delta t/2)} \Delta t \end{aligned} \quad (4)$$

where θ = rotation of block about centroid; and x_i = coordinates of block centroid.

The new position of the block induces new conditions at block boundaries and thus new contact forces. Resultant forces and moments are used to calculate linear and angular accelerations of each block. The calculation scheme summarised above by Eq. (1) to Eq. (4) is repeated until a satisfactory state of equilibrium or continuing failure is reached for each block. It should be noted that time has no real physical meaning if a static analysis was performed. Damping is utilised in the above equations. However, different methods were used for static and dynamic analysis.

If the blocks are deformable, they will be internally discretised into finite difference triangular elements first before the equations of motion are formulated at each gridpoint. The details are discussed in section 3.2.

3. Micro-modelling of unreinforced masonry

3.1 Constitutive laws and failure criterion of joints

Micro modelling of masonry has to consider all basic types of failure mode including both mortar joints and the unit. In general, all tensile and shear damage have been assumed to take place in the relatively weak joints which has been proved to be true for most masonry shear wall panels. The mortar joints are represented numerically as a contact surface formed between two block edges. The constitutive laws applied to the contacts are:

$$\Delta\sigma_n = k_n\Delta u_n \quad (5)$$

$$\Delta\tau_s = k_s\Delta u_s \quad (6)$$

where k_n and k_s are the normal and shear stiffness of the contact, $\Delta\sigma_n$ and $\Delta\tau_s$ are the effective normal and shear stress increments, and Δu_n and Δu_s are the normal and shear displacement increments.

Stresses calculated at grid points located along contacts are submitted to the selected failure criterion. For unreinforced masonry shear wall panels, the Coulomb friction is formulated:

$$|\tau_s| \leq C + \sigma_n \tan \phi = \tau_{\max} \quad (7)$$

where C is the cohesion and ϕ is the friction angle.

There is also a limiting tensile strength f_t for the joint. If the tensile strength is exceeded, then $\sigma_n = 0$.

Joint dilation may also occur at the onset of slip (non-elastic sliding). Dilation is governed in the Coulomb friction model by a specified dilation angle, ψ which measures the uplift of one unit over the other upon shearing. Generally the dilation angle depends on the level of the normal stress, see Fig. 2. For low normal stress, the average value of $\tan\psi$ falls in the range from 0.2 to 0.7, depending on the roughness of the unit surface. The accumulated dilation is limited by either a high normal stress level or by a large accumulated shear displacement. This limitation on dilation corresponds to the observation that crushing of asperities at high normal stress or large shearing would eventually prevent the joint from dilating (Itasca 2000).

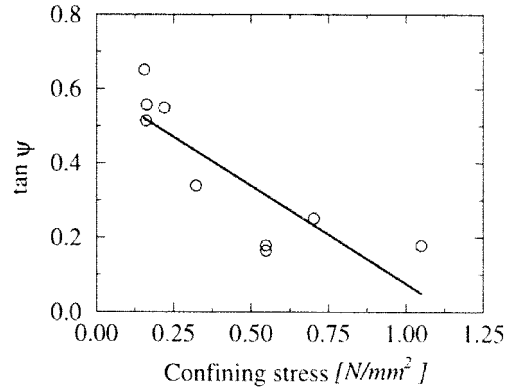


Fig. 2 Effect of normal stress on the dilation angle (Pluijm 1993)

For the joint failure model, the dilation is restricted as follows:

$$\text{if } |\tau_s| \leq \tau_{\max}, \text{ Then } \psi = 0 \quad (8)$$

and

$$\text{if } |\tau_s| = \tau_{\max} \text{ and } |u_s| \geq u_{cs}, \text{ then } \psi = 0 \quad (9)$$

where u_{cs} is critical shear displacement.

3.2 Internal deformation of blocks

In order to calculate the internal deformation of blocks, the deformable blocks have to be discretised into finite difference triangular elements first. The use of triangular elements eliminates the problem of hourglass deformation that may occur with constant-strain finite difference quadrilaterals. Newton's second law is then applied at each grid point. Thereafter, the finite differences technique is used again to calculate velocity and strain at each grid point.

The equations of motion for each grid point are formulated as follows:

$$\frac{\partial u_i^{(t)}}{\partial t} = \frac{\int \sigma_{ij} n_j ds + F_i^{(t)}}{m} + g_i \quad (10)$$

where s is the surface enclosing the mass m lumped at the grid point, n_j is the unit normal to s , $F_i^{(t)}$ is the resultant of all external forces applied to the grid point and g_i is the gravitational acceleration.

A net nodal force vector, $\Sigma F_i^{(t)}$ is calculated at each grid point. This vector includes contributions from applied loads and from body forces due to gravity. If the body is at equilibrium, $\Sigma F_i^{(t)}$ on the node will be zero; otherwise, the node will be accelerated according to the finite difference form of Newton's second law of motion (Eq. 3).

During each time step, strains and rotations are related to nodal displacements in the usual form:

$$\begin{aligned}\dot{\epsilon}_{ij} &= \frac{1}{2}(\dot{u}_{i,j} + \dot{u}_{j,i}) \\ \dot{\theta}_{ij} &= \frac{1}{2}(\dot{u}_{i,j} - \dot{u}_{j,i})\end{aligned}\quad (11)$$

Then the selected constitutive law for the blocks is used to determine stresses at each grid point. For the present study, the relation of stress to strain in incremental form is expressed by Hooke's law in plane stress as:

$$\begin{aligned}\Delta\sigma_{11} &= \beta_1\Delta e_{11} + \beta_2\Delta e_{22} \\ \Delta\sigma_{22} &= \beta_2\Delta e_{11} + \beta_1\Delta e_{22}\end{aligned}\quad (12)$$

where $\beta_1 = E/(1 - \nu^2)$ and $\beta_2 = \nu E/(1 - \nu^2)$

$$\Delta e_{ij} = \frac{1}{2}\left[\frac{\partial \dot{u}_i}{\partial x_j} + \frac{\partial \dot{u}_j}{\partial x_i}\right]\Delta t\quad (13)$$

where Δe_{ij} is the incremental strain tensor, \dot{u}_i is the displacement rate and Δt is time step.

Modelling direct tensile splitting of brick is a more delicate subject (Lourenco 1996). In order to simplify the problem, the brick unit material is modelled with Mohr-Coulomb failure criterion with tension cutoff. The shear flow rule is non-associated and the tensile flow rule is associated. The failure envelope is shown in Fig. 3. From point A to point B, the Mohr-Coulomb yield function is defined as (Itasca 2000):

$$F^s = \sigma_1 - \sigma_2 N_\phi + 2c\sqrt{N_\phi}\quad (14)$$

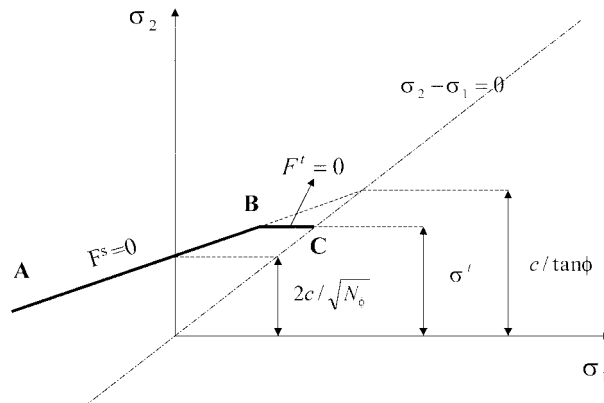


Fig. 3 Mohr-Coulomb failure criterion

and from B to C a tension yield function is defined as:

$$F^t = \sigma^t - \sigma_2 \quad (15)$$

where ϕ is the friction angle, C is the cohesion, σ^t is the tensile strength and

$$N_\phi = \frac{1 + \sin \phi}{1 - \sin \phi} \quad (16)$$

For a material with friction, $\phi \neq 0$ and the tensile strength of the material can not exceed the value σ_{\max}^t given by:

$$\sigma_{\max}^t = \frac{c}{\tan \phi} \quad (17)$$

The shear potential function g^s corresponds to a non-associated flow rule and has the form

$$g^s = \sigma_1 - \sigma_2 N_\psi \quad (18)$$

where ψ is the dilation angle and

$$N_\psi = \frac{1 + \sin \psi}{1 - \sin \psi} \quad (19)$$

The associated flow rule for tensile failure is derived from the potential function g^t

$$g^t = -\sigma_2 \quad (20)$$

In Lourenco (1996) finite element model, a rather simplified method was employed to simulate the tensile splitting of the brick where it was assumed that all damage will occur in the relatively weak joints and, if necessary, in potential pure tension cracks in the units placed vertically in the middle of each unit. The method has also been used in the current research and it has proved the results are quite similar in predicting the failure pattern of the masonry walls.

4. Numerical examples

All the numerical examples presented in this paper were performed with the numerical code UDEC (Itasca 2000). Numerical modelling cannot be proved until the results are compared with those obtained from experiments. In the literature, there are a lot of experimental results on shear walls. However, most tests were conducted at macro scales, the material properties and other testing data of mortar joints were ignored. In order to better understand the behaviour of masonry and provide testing data for the micro-modelling of masonry using finite element method, a series of experiments were carried out in the Netherlands. Some tests were conducted at the micro level with a full set of results for mortar joints (Lourenco 1996). These testing results are used to validate the numerical model discussed in this paper which is based on the Distinct Element Method.

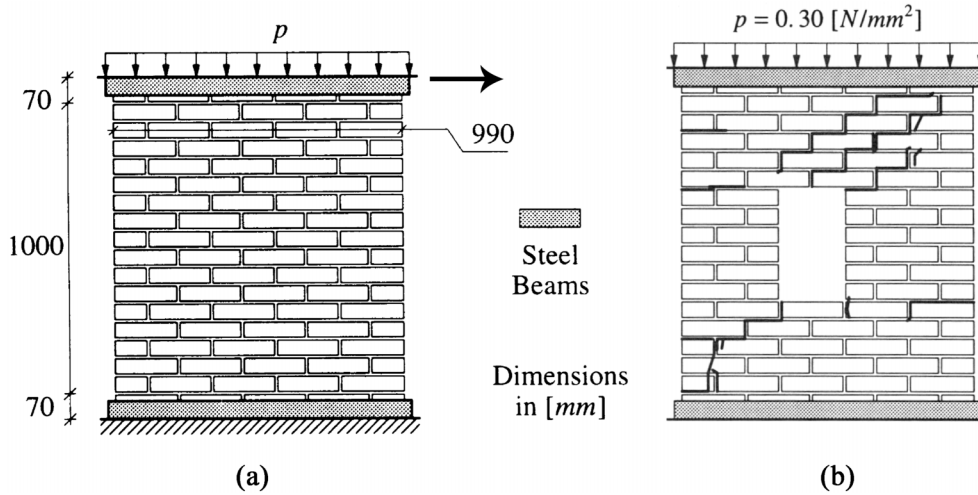


Fig. 4 Experimental shear wall set-up: (a) wall without opening; (b) wall with a central opening (Lourenco 1996)

Table 1 Summary of elastic material properties

Brick		Joint	
E (MPa)	ν	k_n (N/mm ³)	k_s (N/mm ³)
16700	0.15	82	36

where k_n is joint normal stiffness and k_s is joint shear stiffness.

Table 2 Summary of joint inelastic properties

Tension		Shear	
f_t (N/mm ²)	$\tan\phi$	$\tan\psi$	C (MPa)
0.25	0.75	0.0	0.375

4.1 Summary of experiment set-up

The shear wall panel has a width/height ratio of 990 mm × 1000 mm, built up with 18 courses with and without a central opening, as shown in Fig. 4. The wall is made of wire-cut solid clay bricks with dimensions 210 mm × 52 mm × 100 mm and 10 mm thick mortar. The wall was subjected to a vertical compressive stress $\sigma_m = 0.3$ MPa. During testing, a horizontal displacement was monotonically increased until failure.

Before full-scale wall testing was performed, some micro-scale experiments were conducted to determine the material properties of both the bricks and mortar joints. These material properties are listed in Tables 1 and 2.

4.2 Comparison of numerical and experimental results

Due to the effect of mortar joints, masonry should be analysed as a discontinuous system. Both the behaviour of the discontinuities and the behaviour of the solid material have to be considered. In the following numerical study, the discontinuous media is represented as an assemblage of discrete blocks. The mortar joint is represented numerically as a contact surface formed between two block edges and the contact may be considered as a boundary condition which applies external forces to each block. The triangular element mesh used in the analysis is shown in Fig. 5.

4.2.1 Walls without opening

During the experiment, two horizontal tensile cracks develop at the bottom and top of the walls at an early loading stage due to lower value of vertical load, and a stepped diagonal crack through head and bed joints immediately follows. Under increasing deformation, the crack progresses in the direction of the supports and finally a collapse mechanism is formed (Lourenco 1996). Such behaviour of the wall has been successfully reproduced by the numerical model using DEM. The experimental crack pattern is shown in Fig. 6(a). Fig. 6(b) shows the finite element results of the final failure pattern of the wall (Lourenco 1996). The tensile and shear cracks development and the progressive failure of the wall modelled by the authors using DEM are indicated in Fig. 7. It can be seen from above figures, the behaviour of the wall is well captured by the proposed model.

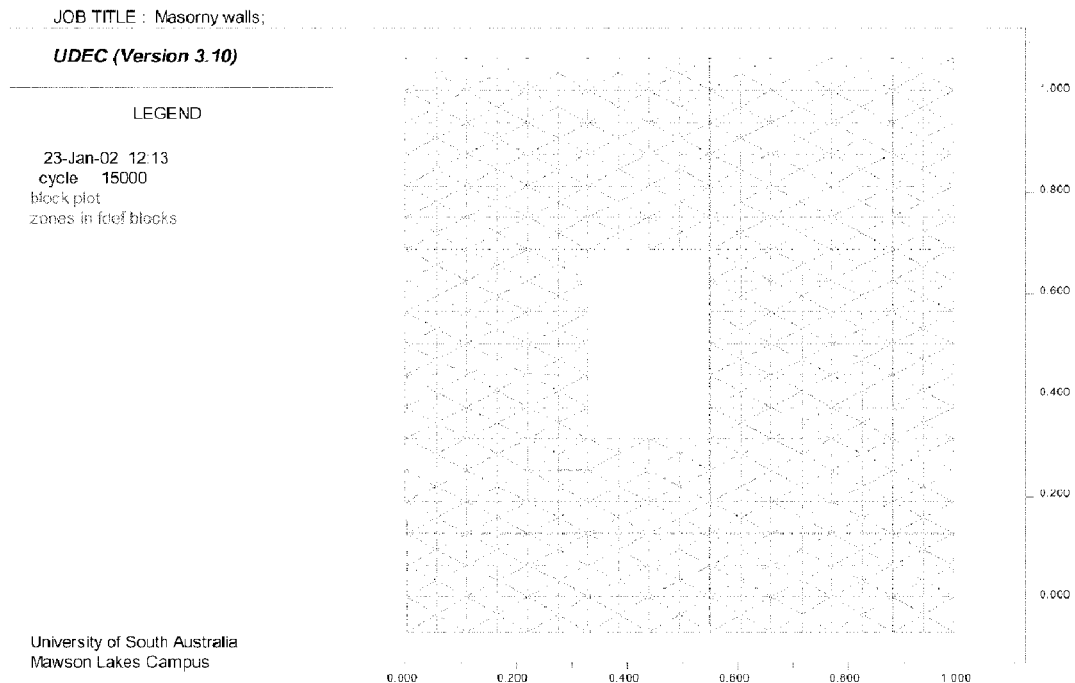


Fig. 5 The triangular element mesh for masonry wall

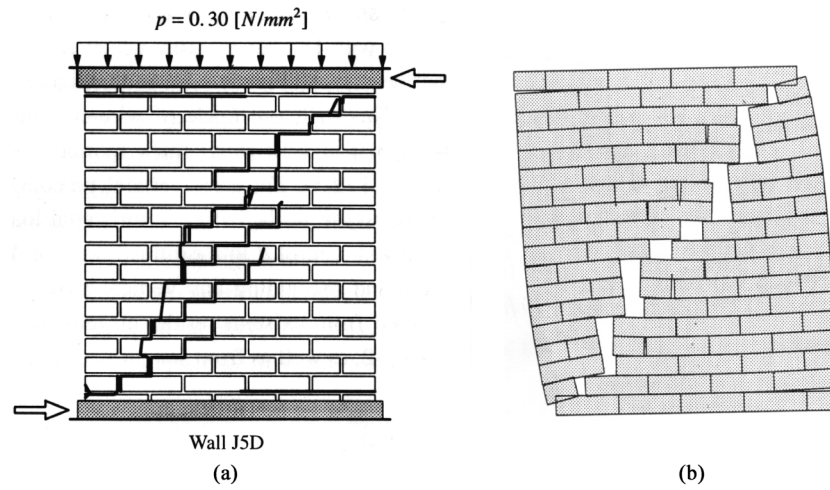


Fig. 6 Experimental and finite element results of crack and failure patterns: (a) experimental crack; (b) finite element prediction of the final failure pattern (Lourenco 1996)

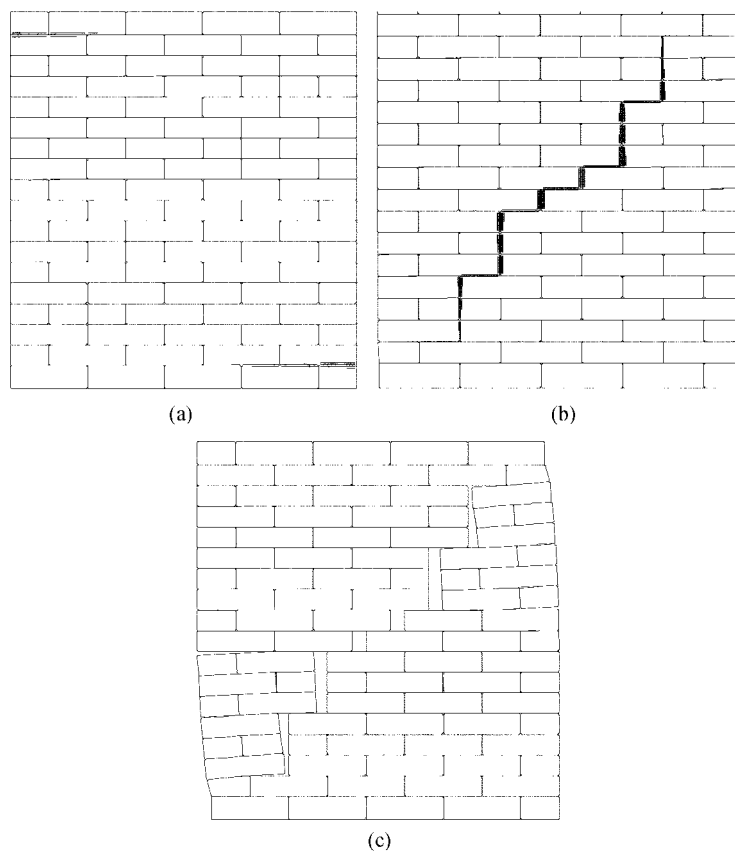


Fig. 7 Crack and failure patterns of the analysis using DEM: (a) at a displacement of 1.0 mm; (b) at a displacement of 2 mm; (c) final failure pattern

The principal stress distribution at different loading stages has also been compared between finite element modelling proposed by Lourenco (1996) and distinct element modelling by the current research (see Figs. 8 and 9). At the early stage, due to the different stiffness of joints and bricks, small struts are oriented parallel to the diagonal line defined by the centre of the bricks, see Figs. 8(a) and 9(a). Finally, when the diagonal crack is fully open, two distinct struts are formed, one at each side of the diagonal crack, see Figs. 8(b) and 9(b). This comparison further proved the abilities of the distinct element modelling.

It can be seen that the maximum compressive stress occurred at the bottom corner of the wall which indicates the potential toe crushing. The maximum tensile stress developed in the bricks follows the same path of the final diagonal cracks which indicates the potential cracks in the bricks when the final diagonal stepped failure occurs.

4.2.2 Walls with a central opening

The second example concerns the wall has the same geometry, loading conditions and material properties as for example one, but with a central opening as shown in Fig. 4(b).

The central opening of the wall produces two small weak piers. During the experiment, diagonal zigzag cracks arise initially from two corners of the opening at four possible locations and then tensile cracks arise from the outside of the wall at the base and top of the small piers, as shown in Fig. 10(a). Finally, a collapse mechanism is formed with failure of the compressed toes, located at the bottom and top of the wall and at the bottom and top of the small piers (see Fig. 10(b)). The cracks shown in Fig. 10(b) remain active and the wall behaves similarly to four rigid connected by the hinges shown (Lourenco 1996). The final failure pattern predicted by the finite element model is shown in Fig. 10(c).

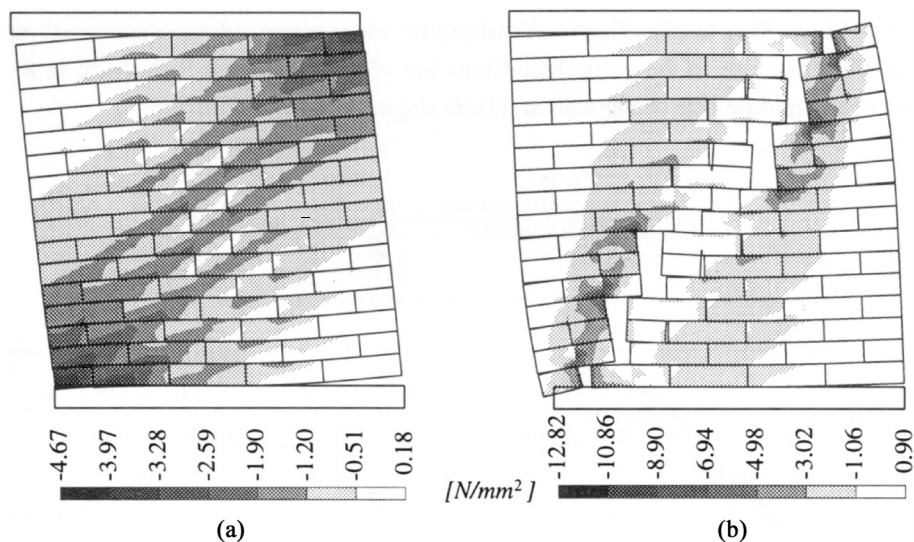
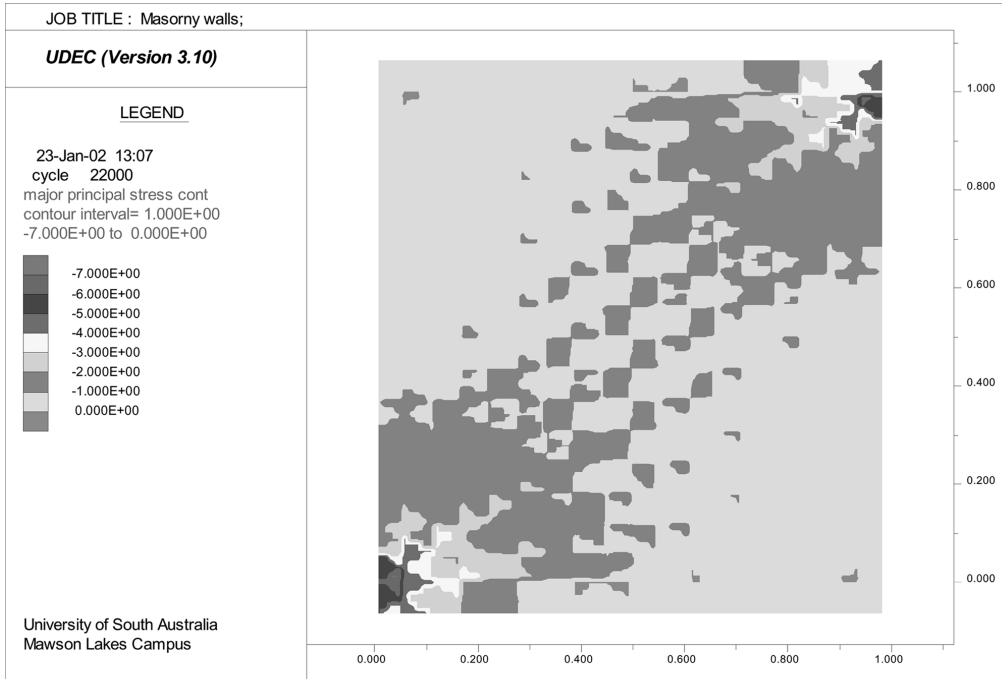
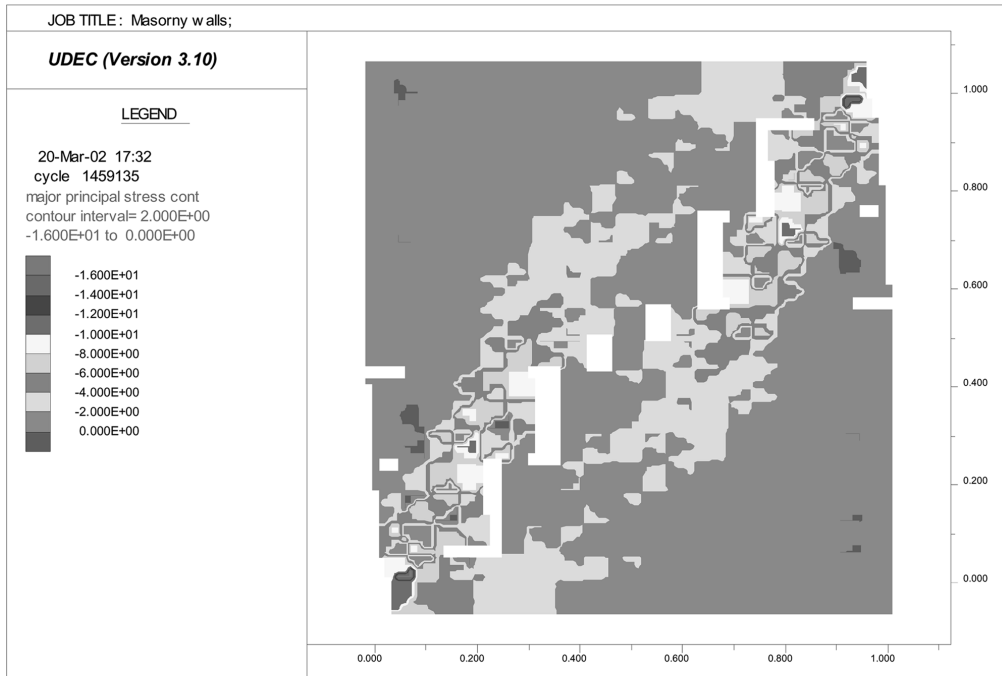


Fig. 8 Principal stress distribution from FEM at a displacement of: (a) 1.0 mm and (b) 4.0 mm (Lourenco 1996)



(a)



(b)

Fig. 9 Principal stress distribution from DEM at a displacement of: (a) 1.5 mm and (b) 4.5 mm

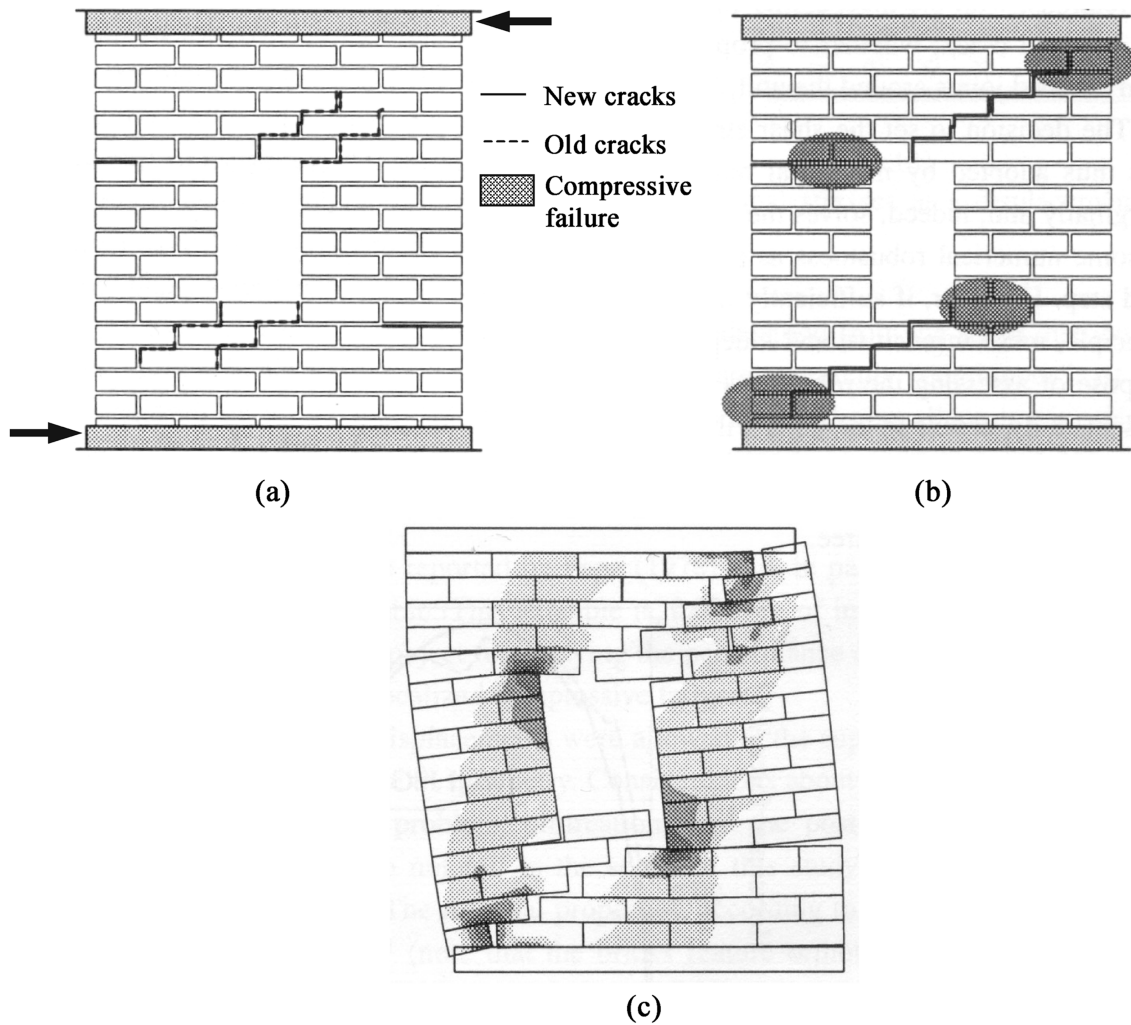


Fig. 10 Experimental and finite element crack and failure pattern of the wall panel: (a) initial diagonal cracks and horizontal tensile cracks in small piers, (b) collapse mechanism with four hinged rigid blocks, (c) finite element prediction of the final failure pattern (Lourenco 1996)

In general, the numerical model using DEM captures well the experimental behaviour discussed above, as demonstrated in Fig. 11. Initially, diagonal zigzag cracks arise from the corner of the opening. Then horizontal cracks appear in the bottom and in the top of the small piers, see Fig. 11(a). Under increased loading conditions, these cracks were further progressed and developed to the compressed toes (Fig. 11(b)). The final failure mode is illustrated in Fig. 11(c), it shows a good agreement with experiment and finite element analysis results. The final collapse is indicated when the iteration failed to reach equilibrium.

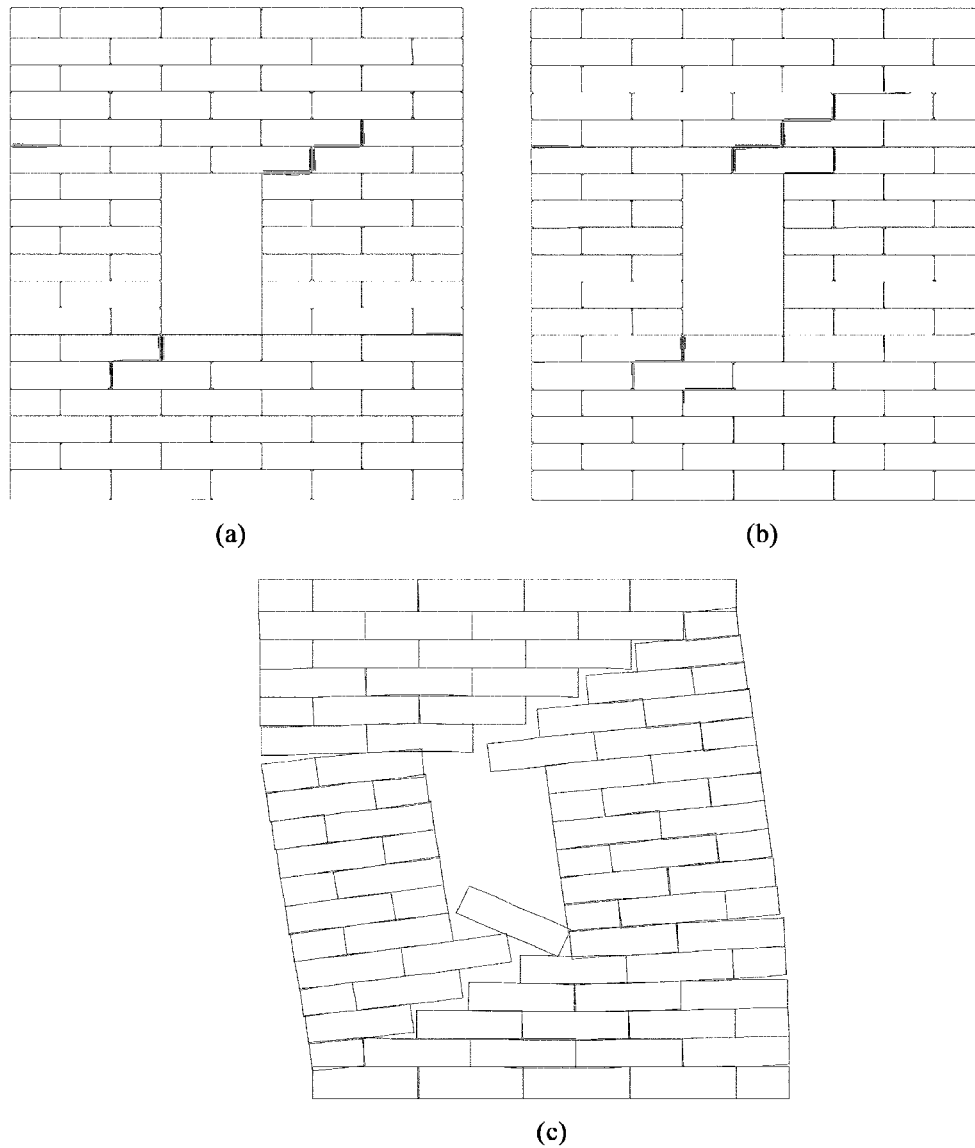
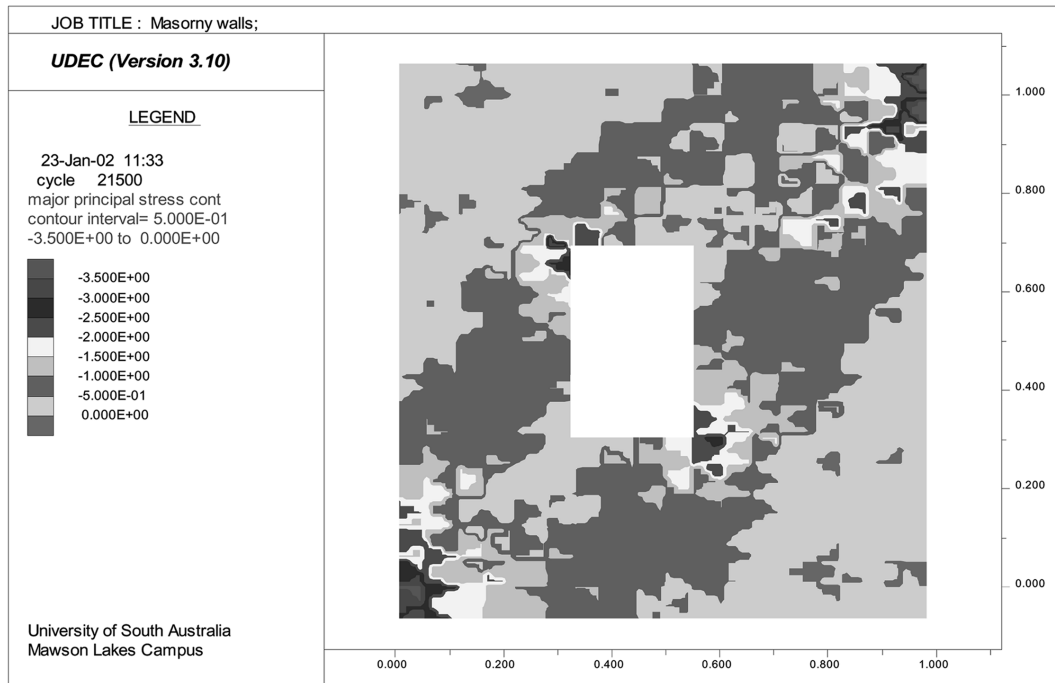
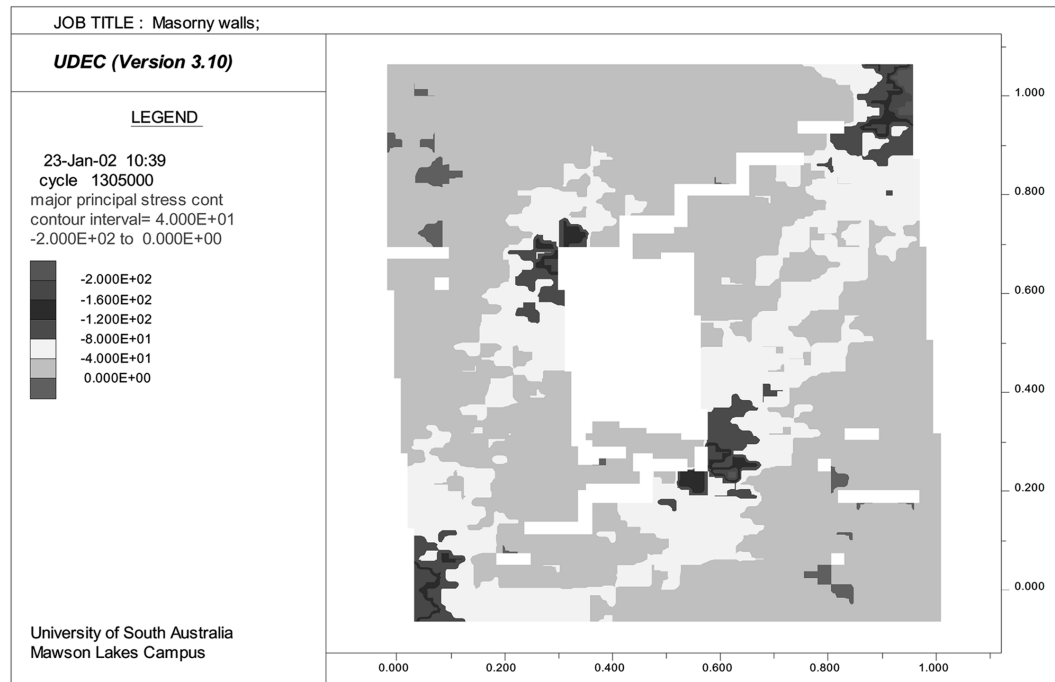


Fig. 11 Numerical modelling of the crack and failure patterns of the wall panel using DEM: (a) initial diagonal cracks and horizontal tensile cracks in small pier, (b) cracks development, (c) wall failure pattern at peak load

Fig. 12 shows the DEM analysis results of the distribution of minimum principal stresses. It can be seen from the figure that two compressive struts have formed. It is clearly indicated the locations of the maximum compressive stresses which is agreed well with the testing results (Fig. 10(b)). The DEM model captures the locations of the maximum compressive stresses at the top and bottom of the wall as well as the top and the bottom of the small piers.



(a)



(b)

Fig. 12 DEM results of minimum principal stresses: (a) at a displacement of 1 mm (b) at peak load

5. Conclusions

Masonry is not a simple material, the influence of mortar joints as a plane of weakness is a significant feature. Due to the nature of the problem, two-phase micro-modelling of brick and mortar is required. However, this makes the numerical modelling of masonry very complex. This paper has discussed an alternative and simple way of modelling masonry, which is using the Distinct Element Method. The preliminary results obtained in the current research have shown the great potential of the method, especially for dynamic analysis. It has been demonstrated in the paper, that both the tensile and shear failure of the mortar joints, could be captured by the model, as well as the final collapse mechanisms of the whole masonry shear panel. The results compared well with those obtained from experiments and a sophisticated finite element model.

Further study should be conducted into the prediction of the final failure load. It has been found the results pertaining to the failure load may not be stable when a static analysis is performed.

References

- Cundall, P.A. (1971), "A computer model for simulating progressive large scale movements in blocky rock systems", *Proc. of the Sym. of the Int. Society for Rock Mechanics*, Nancy, France, **1**(II-8), 11-18.
- Dhanasekar, M. (1985), "The performance of brick masonry subjected to in-plane loading", PhD Thesis, The University of Newcastle, NSW, Australia.
- Dialer, C. (1992), "A distinct element approach for the deformation behaviour of shear stressed masonry panels", *Proc. of the 6th Canadian Masonry Symposium*, Saskatchewan, Canada, 765-776.
- Formica, G., Sansalone, V. and Casciaro, R. (2002), "A mixed solution strategy for the nonlinear analysis of brick masonry walls", *Comput. Meth. Appl. Mech. Eng.*, **191**(51-52), 5795-6044.
- Gambarotta, L. and Lagomarsino, S. (1997a), "Damage models for the seismic response of brick masonry shear walls. Part I: the mortar joint model and its applications", *Earthq. Eng. Struct. Dyn.*, **26**, 423-439.
- Gambarotta, L. and Lagomarsino, S. (1997b), "Damage models for the seismic response of brick masonry shear walls. Part II: the continuum model and its applications", *Earthq. Eng. Struct. Dyn.*, **26**, 441-462.
- ITASCA Consulting Group (2000), "Universal distinct element code", *ITASCA Consulting Group, Inc.*, Minneapolis, Minnesota, USA.
- LaRovere, H. (1990), "Nonlinear analysis of reinforced concrete masonry walls under simulated seismic loadings", PhD Thesis, University of California, San Diego, U.S.A.
- Lotfi, H. and Shing, P. (1994), "Interface model applied to fracture of masonry structure", *J. Struct. Engrg.*, ASCE, **120**, 63-80.
- Lourenco, P.B. (1996), "Computational strategies for masonry structures", PhD Thesis, Delft University of Technology, The Netherlands.
- Page, A. (1978), "Finite element model for masonry", *J. Struct. Div.*, ASCE, **104**(8), 1267-1285.
- Pluijm, R. Van Der (1993), "Shear behaviour of bed joints", *Proc. of the 6th North American Masonry Conf.*, eds. Hamid, A.A. and Harris, H.G., Drexel University, Philadelphia, Pennsylvania, USA, 125-136.
- Psycharis, I., Papastamatiou, D. and Alexandris, A. (2000), "Parametric investigation of the stability of classical columns under harmonic and earthquake excitations", *Earthq. Eng. Struct. Dyn.*, **29**, 1093-1109.
- Vratsanou, V. (1991), "Determination of the behaviour factors for brick masonry panels subjected to earthquake actions", *Proc. of the Int. Conf. on Soil Dynamics and Earthquake Engineering*, Germany: 23-26.
- Zhuge, Y. (1998), "Distinct element modelling for masonry dam under earthquake load", *Proc. of the 5th Australasian Masonry Conf.*, Gladstone, Australia, 435-442.
- Zhuge, Y. (1999), "Distinct element modelling of unreinforced masonry walls", *Proc. of the 7th East Asia-Pacific Conf. on Structural Eng. Construction*, Kochi, Japan, 411-416.
- Zhuge, Y., Thambiratnam, D.P. and Corderoy, J. (1998), "Nonlinear dynamic analysis of unreinforced masonry", *J. Struct. Eng.*, ASCE, **124**(3), 270-277.